

# Tracking El Niño using optical indices of phytoplankton dynamics in the equatorial Pacific

Joel Craig<sup>1</sup>, Pete Strutton<sup>2</sup>, Wiley Evans<sup>2</sup>

1. College of Earth and Atmospheric Science, Georgia Institute of Technology, Atlanta, Georgia

2. College of Oceanic and Atmospheric Science, Oregon State University, Corvallis, Oregon

## Abstract

In situ and satellite measures of various ocean and atmospheric parameters are used to understand ecosystem dynamics. Lab tests have modeled the response of various wavelengths of light to particulate matter of varying sizes and consistencies in water. Ratios of chlorophyll to carbon change with species and light availability. Optical measures of fluorescence are used to measure chlorophyll. Backscatter and beam attenuation can be used as proxies for particulate organic carbon (POC). Using recently collected equator transect optical data calibrated with bottle measures of chlorophyll and particulate organic carbon (POC) concentrations we seek to model ecosystem dynamics using a less labor intensive approach.

## Introduction

During El Niño events the eastern trade winds in the equatorial Pacific weaken and then reverse causing Kelvin waves to propagate eastward across the open ocean. These Kelvin waves are trapped on the equator by coriolis and cause downwelling. This causes the normal upwelling in the east to decrease and the thermocline, which is normally tilted and shallow in the eastern Pacific, to flatten out. This slackening wind also causes Rossby waves to propagate westward causing the western Pacific's normally deep thermocline to shoal. Subsequently, the tongue of cold water normally extending out from the west coast of South America is diminished or non-existent. Without this westward movement of water along the surface, the Equatorial under current (EUC) also slackens and flattens out in conjunction with the thermocline. During the

1997-1998 El Niño event the initial anomalous westerly wind events came in bursts from the western Pacific caused by the Madden-Julian Oscillation. These bursts continued long enough to force the western Pacific warm pool east and shut down upwelling entirely to the coast of South America. These bursts stopped, and thus stopped the downwelling Kelvin waves, before normal trade winds resumed. During this time the eastern thermocline shoaled to more normal levels; then, as cold nutrient rich waters were already near the surface, when easterly trade winds resumed, upwelling began again and caused a drastic spike in surface nutrients and chlorophyll (Strutton and Chavez, 2000).

The coriolis induced upwelling along the equator results in moderate concentrations of macronutrients, and thus a higher concentration of phytoplankton relative to the adjacent oligotrophic gyres. However phytoplankton growth is lower than expected given the concentration of macronutrients present in the surface water owing to growth-limiting concentrations of iron (Chavez, 1999).

Since 1988 data on wind velocity, temperature through the upper 500 m, air temperature and relative humidity have been collected by the Tropical Atmosphere Ocean (TAO) project array of around 70 buoys tracing meridians from 156E to 95W between 8N and 8S (Figure 1). Since 1996 cruises have traced the buoy lines twice a year taking CTDs, water column samples and performing maintenance on the buoys. In 2005 the CTD rosette was fitted with a chlorophyll fluorometer, backscattering meter and C-star beam attenuation meter (proxies for chlorophyll, particulate organic carbon and more!). In 1998 the SeaWiFS satellite came on line to measure chlorophyll and phytoplankton carbon by comparing different wavelengths of reflected light and backscatter.

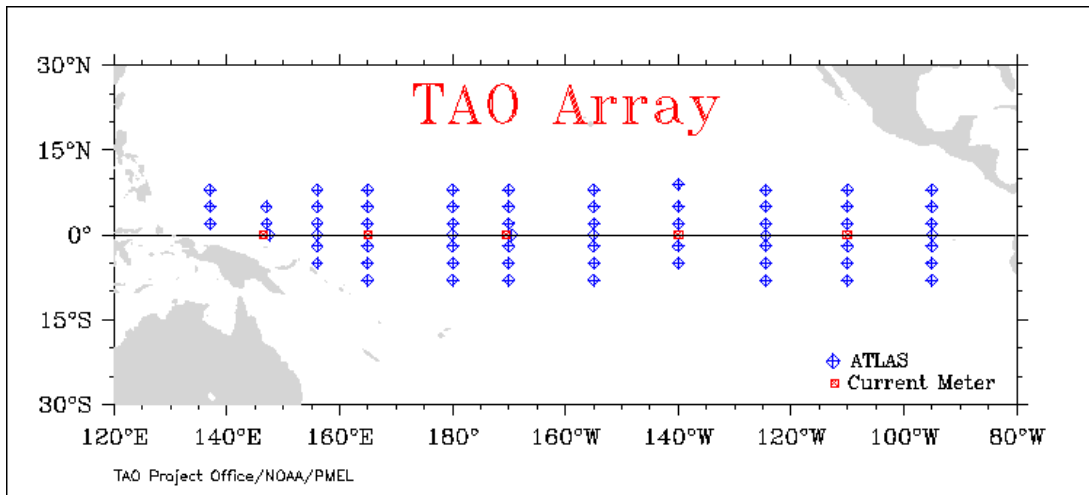


Figure 1. Map of equatorial Pacific showing location of buoys in the TAO array.

## Methods

Chlorophyll fluorescence is a function of chlorophyll concentration, but also varies due to the changing physiological state of phytoplankton under varying light conditions (Figure 2).

Because of this, light availability must be considered along with fluorescence in calculating chlorophyll concentration. A multiple linear regression was performed using fluorescence, depth and time of day leading to a fairly high correlation between the measured bottle chlorophyll data and our predicted values (Figure 3). Both total beam attenuation ( $C_p$ ) and particulate backscatter ( $b_{bp}$ ) can be used as proxies for POC (Figure 4). We chose to use  $b_{bp}$  because a large portion of the transmissometer  $C_p$  data was not useable due to instrument problems (Figure 5). With these instrument calibrations, latitude vs. depth profiles from each transect with bottle data were compiled for bottle measured chlorophyll, calculated chlorophyll, and the ratio between the two (error) (Figure 6). Likewise for bottle and calculated POC (Figure 7).

Satellite data were interpreted according to the literature (Behrenfeld et al., 2005)

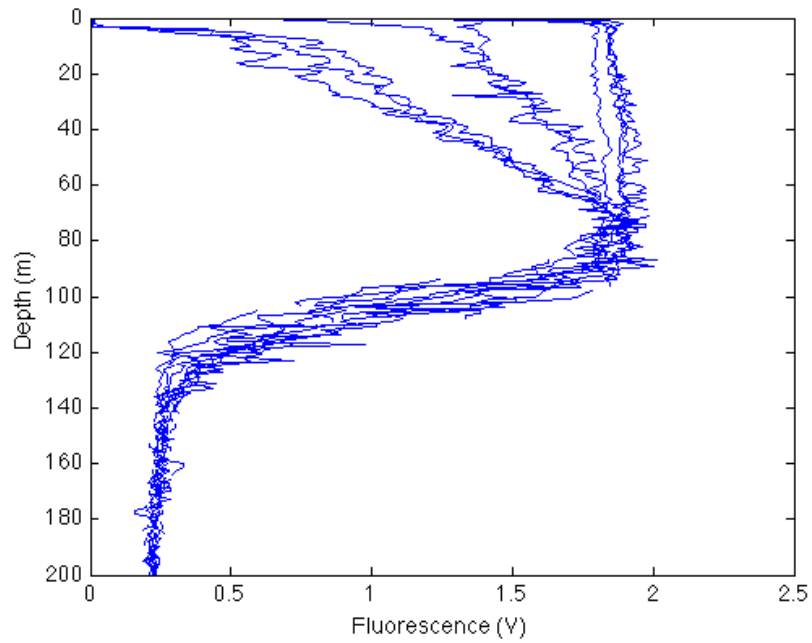


Figure 2. Chlorophyll fluorescence from a stationary point in the equatorial Pacific over a 24-hour period showing an apparent chlorophyll change in the photic zone due to changes in the fluorescence per unit Chl; high relative fluorescence in the daytime and low at night

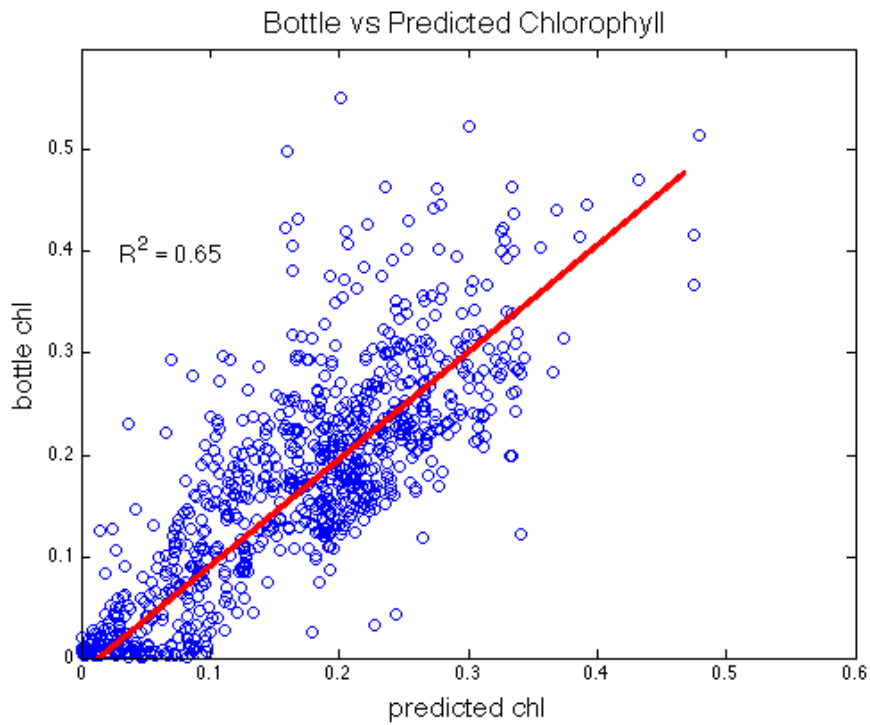


Figure 3. Chlorophyll values predicted by multiple linear regression from fluorescence and light availability (depth and time of day) vs. bottle Chl data showing a fairly high correlation

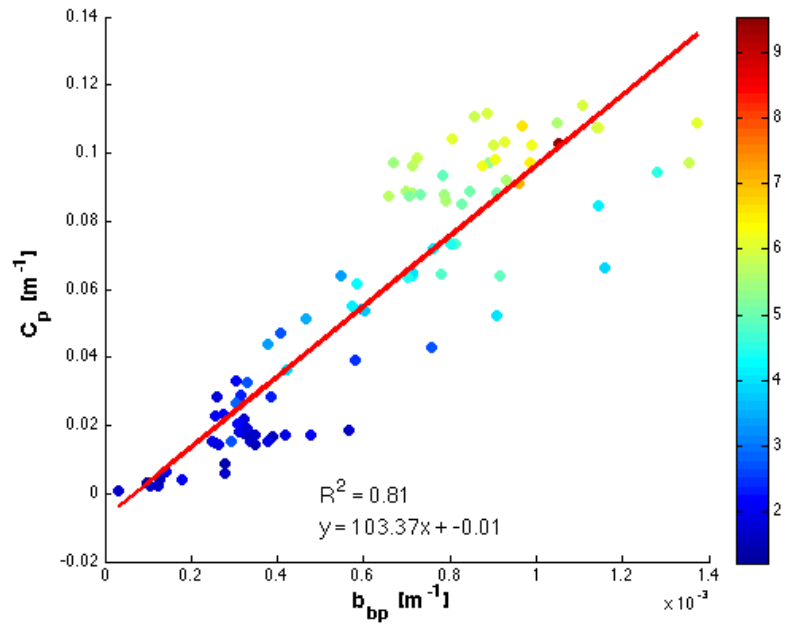


Figure 4. POC concentration vs. particulate backscatter and particulate beam attenuation showing a high correlation between beam attenuation and backscatter

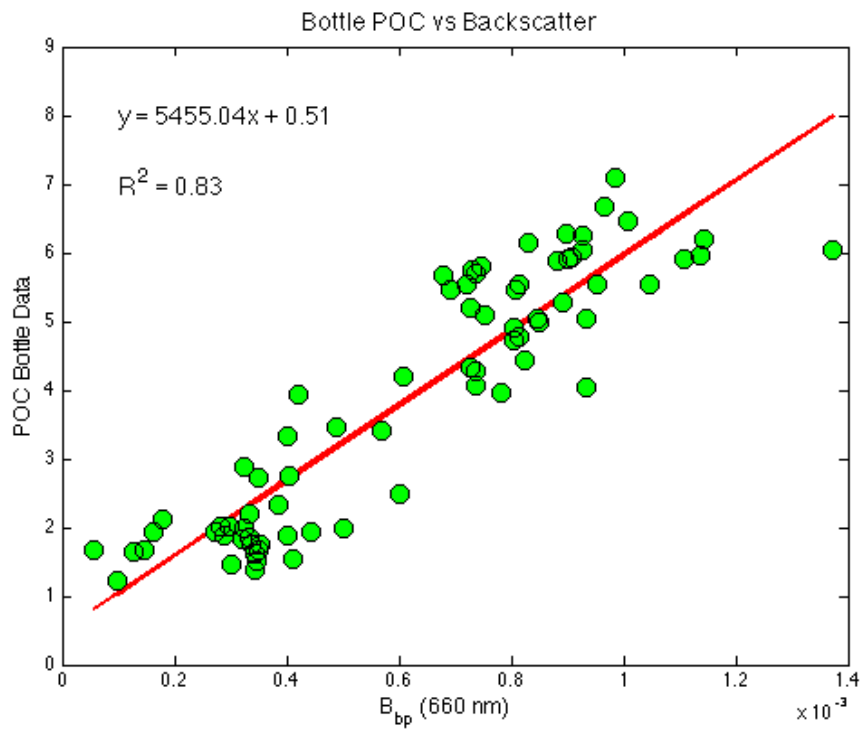


Figure 5. Particulate backscatter vs. concurrent bottle data from two TAO transects (125W & 140W) at depths from 0-200 m showing a high correlation.

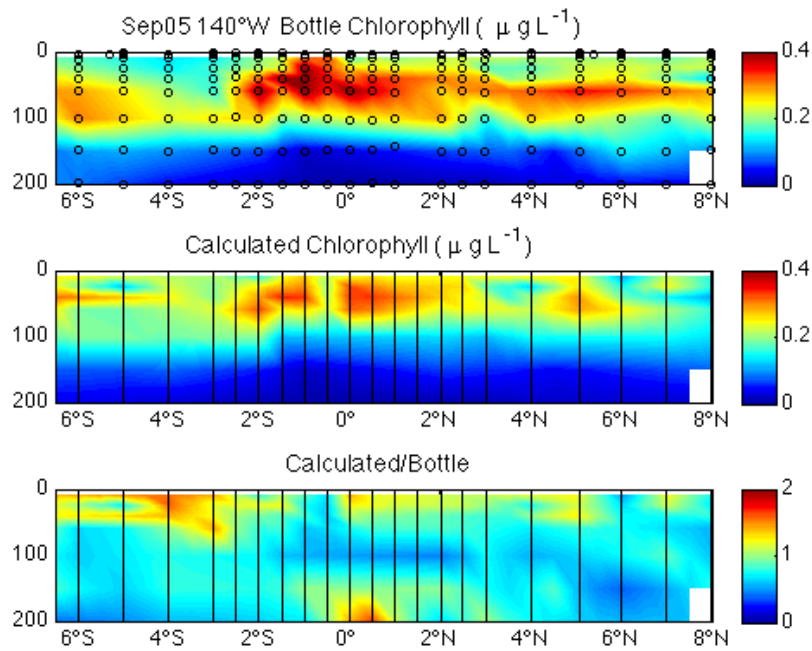


Figure 6. Example of latitude vs. depth plots for bottle measured and concurrent optical data calculated Chl and the ratio between the two (error)

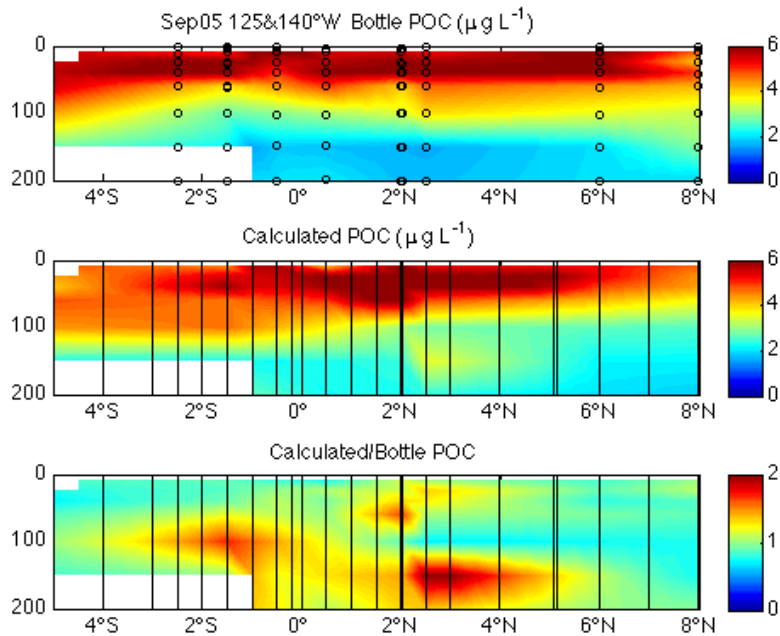


Figure 7. Example of latitude vs. depth plots for bottle measured and concurrent optical data calculated POC and the ratio between the two (error)

## Results

Using these same methods we then processed all transects (34), and compared calculated chlorophyll, calculated POC, and the ratio between the two (Example Figure 8).

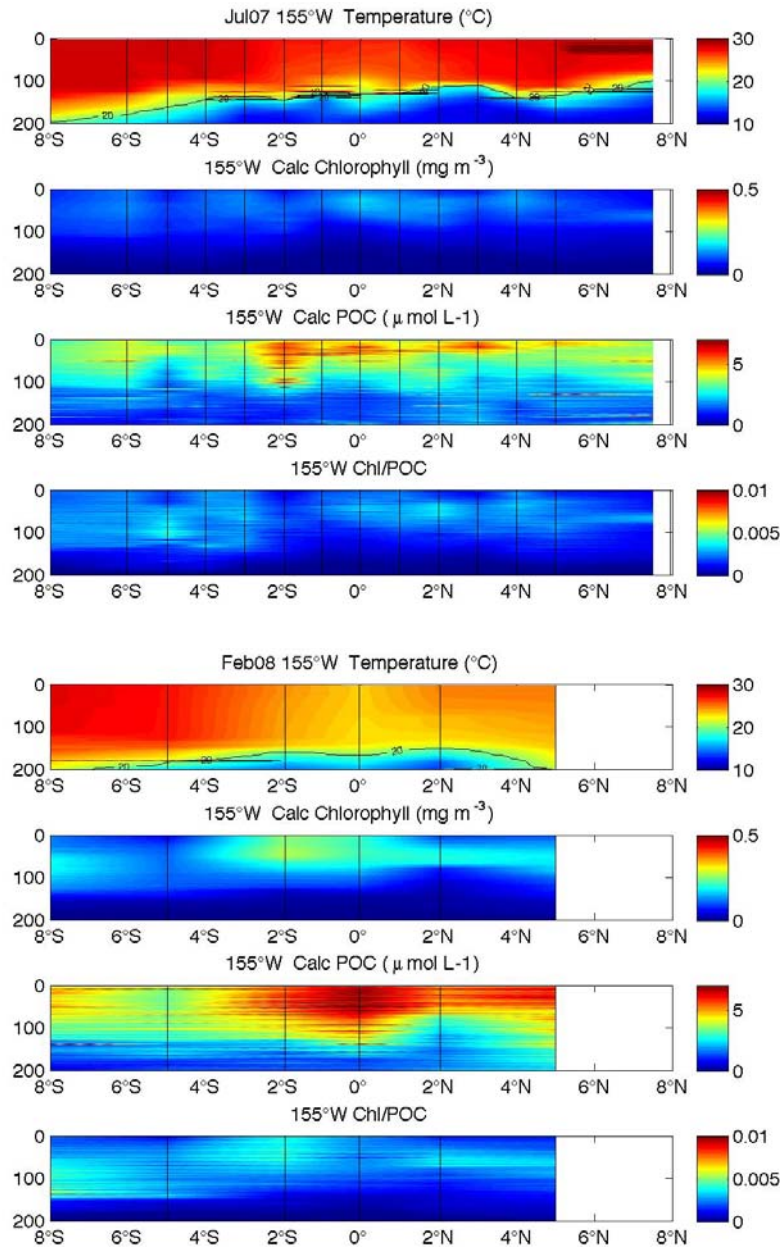


Figure 8. Example latitude vs. depth transects showing temperature, calculated Chl and POC and their ratio (error); top showing low chlorophyll, in reduced upwelling El Niño conditions and bottom showing La Niña equator centered upwelling, temperature minimum, and subsequent chlorophyll and POC maximums.

Monthly mean temperature chlorophyll and phytoplankton carbon were then derived from SeaWiFS satellite data for January 2005 through August 2007 (Example Figure 9).

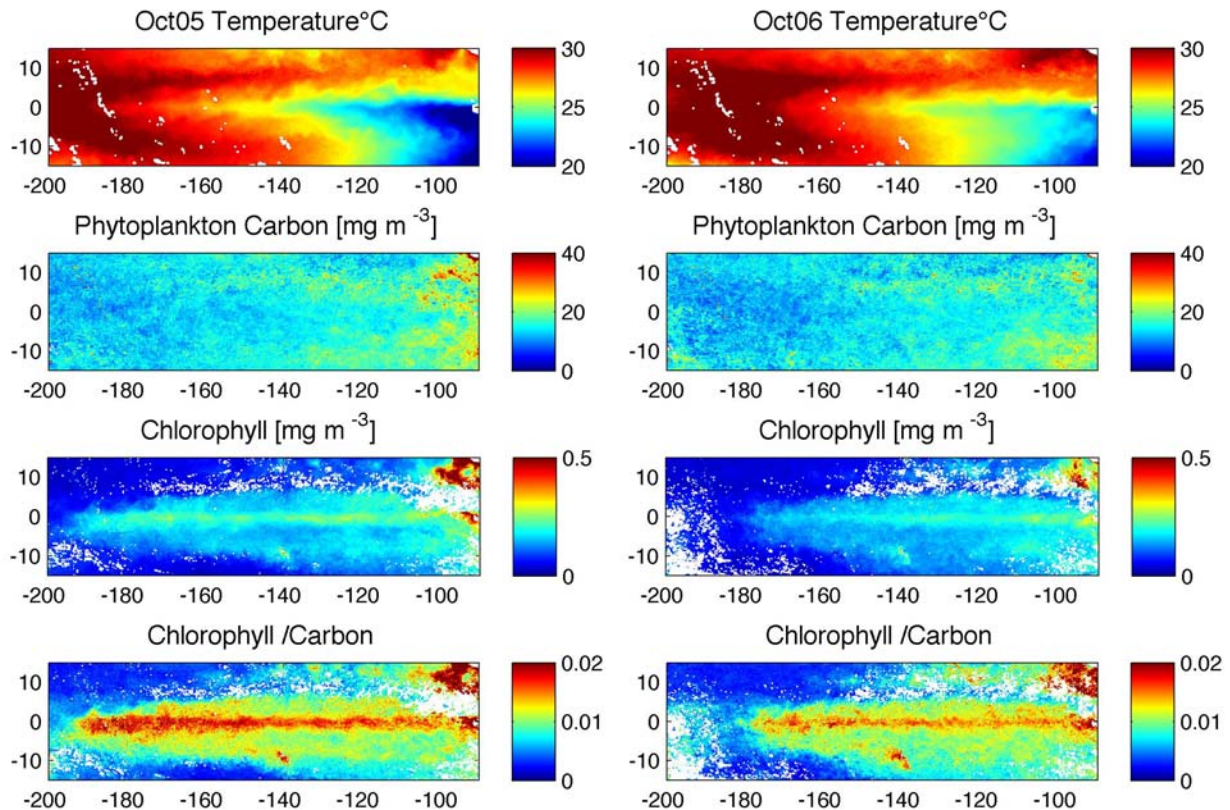


Figure 9. Two examples of longitude vs. latitude monthly mean temperature, phytoplankton carbon, chlorophyll and Chl /carbon; the left showing typical equator centered upwelling, chlorophyll and carbon maximums and the right showing reduced quantities due to El Niño.

During the peak of an El Niño cycle, reduced upwelling causes warmer sea surface temperatures (Figure 10). The reduced nutrient flux to the surface causes decreased phytoplankton growth and thus decreased chlorophyll and measured fluorescence (Figure 11). We observed only a small subsequent decrease in POC in surface waters (Figure 12). Therefore the observed decrease in chl/POC is mostly due to changes in chlorophyll concentrations (Figure 13). For all of these

calculations we consider equatorial surface water to be mean values from the surface down to 20 m between 2S and 2N. This observed decrease in chl/POC may be due to decreased overall primary production. This decrease leads to clearer water and less of a need for the remaining phytoplankton to contain high chlorophyll levels in order to compete for scarce photons (Geider). There also seems to be a relationship between nutrient supply and chl/POC, as iron is needed to make chlorophyll. As well POC may be only 30-50% living autotrophs as this quantity includes heterotrophs and detritus (Peña et al., 1991).

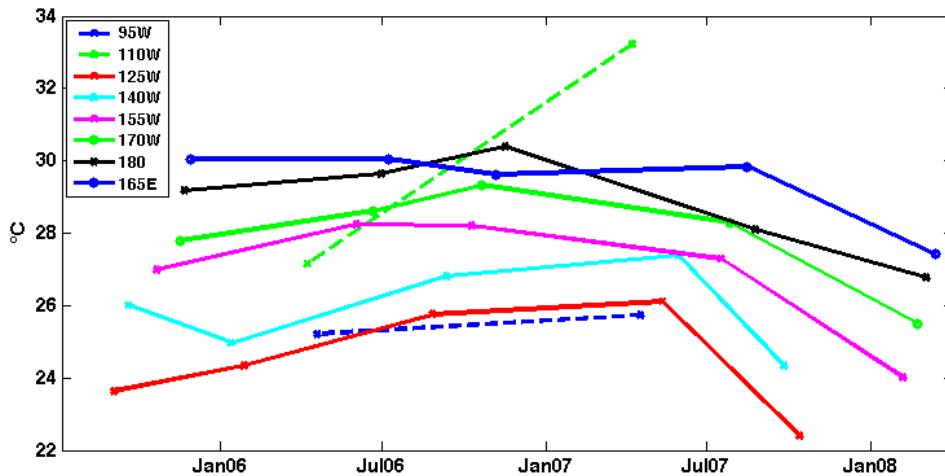


Figure 10. Mean equatorial surface temperature for all TAO lines over time showing a sharp surface temperature drop in the latter half of 2007 as Easterly winds and upwelling resumed.

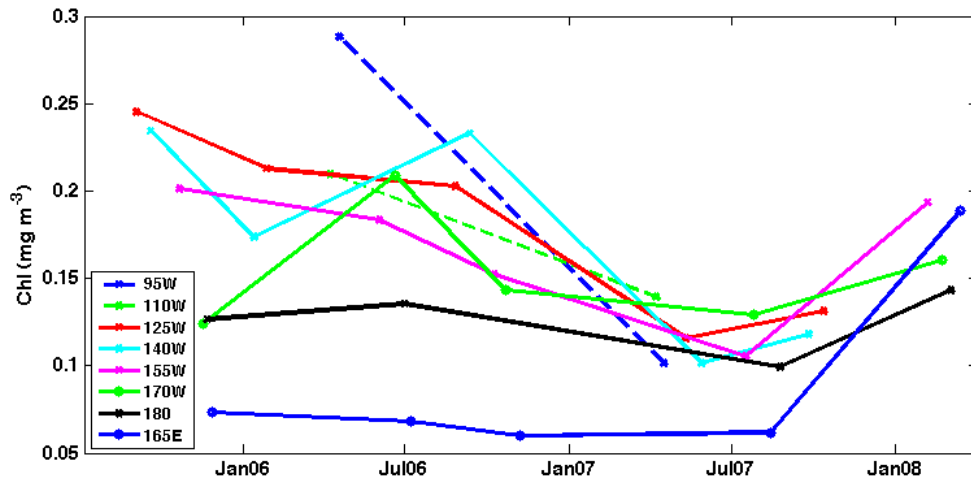


Figure 11. Mean Chlorophyll of equatorial surface waters for all TAO lines over time showing a steep decrease, particularly in the eastern Pacific, as El Niño conditions strengthened and a dramatic increase as conditions returned to normal and further into a La Niña.

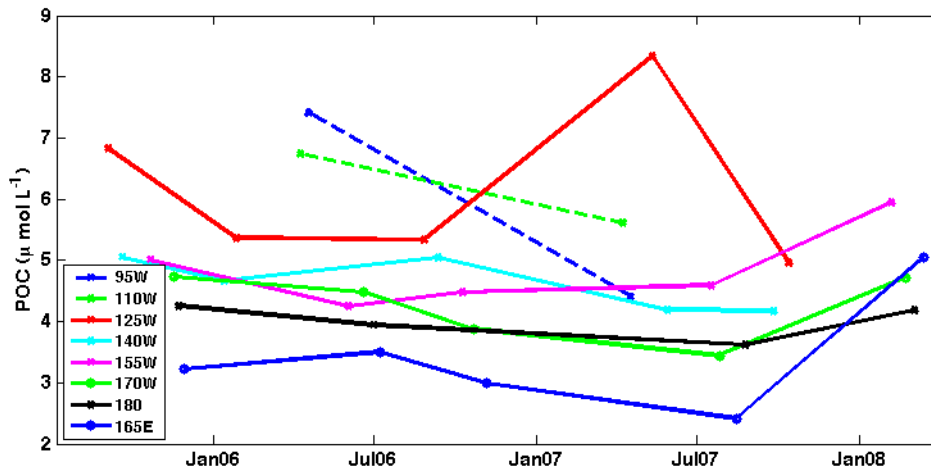


Figure 12. Mean POC of equatorial surface waters for all TAO lines over time showing a slight decrease as El Niño conditions strengthened and a moderate increase as conditions returned to normal and further into a La Niña.

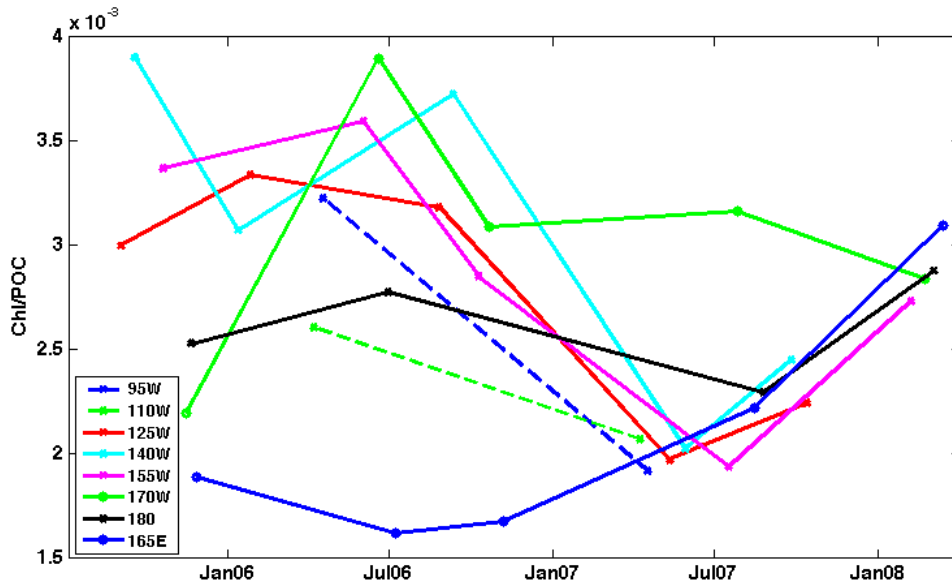


Figure 13. Mean Chlorophyll /POC ratio over equatorial surface waters for all TAO lines over time showing a steep decrease as El Niño conditions strengthened and a dramatic increase as conditions returned to normal and further into a La Niña.

## Conclusions

Optical properties sufficiently model ecosystem changes and there is fairly good agreement between satellite and optical data. These data are less labor intensive to gather and provide finer spatially resolved measurements than do bottle samples. Further work is needed to improve the calibration of instruments and to determine real physical meaning of signals, particularly POC and its non-autotrophic portions.

This work made possible by the CIOSS research group and by the letters S and T.

## References:

- Behrenfeld et al., *Global Biogeochemical Cycles* 19, GB1006 (2005).
- F.P. Chavez et al., *Science* 286, 2126 (1999).
- M. Peña et al., *Marine Ecology Progress Series* 22, 179-188 (1991).
- P.G. Strutton, F.P Chavez, *J. Geophysical Research* 105, C11 (2000).